15th Australasian Fluid Mechanics Conference
The University of Sydney, Sydney, Australia
13-17 December 2004

Dam Break Wave Propagation on Abrupt Drops: an Experimental Study

H. Chanson[1]
[1]Dept of Civil Engineering, The University of Queensland,
Brisbane QLD 4072, AUSTRALIA

Abstract

Flood waves resulting from dam breaks and flash floods have been responsible for numerous losses. In the present study, sudden flood releases were investigated down a large waterway with a succession of abrupt drops. A new experimental technique was developed to obtain instantaneous void fractions, bubble count rates and velocities using arrays of conductivity probes. The surging waters propagated as a succession of free-jets and horizontal runoff flow motion downstream of each abrupt drop. A strong aeration of the surge front was observed for all flow conditions. In the runoff region, instantaneous velocity measurements indicated a turbulent boundary layer region.

Introduction

Surge waves resulting from dam breaks have been responsible for numerous losses of life (Fig. 1A). Related situations include flash floods, debris flow surges, surging waves in the swash zone, rising tides in dry estuaries and tsunami runup on dry land. In all cases, the surge front is a shock characterised by a sudden discontinuity and extremely rapid variations of flow depth and velocity. Despite a few early studies [1,2], current knowledge of dam break wave surging down rough surfaces is rudimentary and the aerated nature of the surging waters remains un-quantified, although clearly evidenced by photographs, movies and witness reports.

Hydraulic researchers have studied surging flows in laboratory facilities, but the findings have been sometimes contradictory. Some researchers highlighted a boundary layer region in the surging wave leading edge, including Mano [3] who studied unsteady wave runup using bubble tracer and high speed video, and Fujima and Shuto [4] who performed steady LDA (1 component) measurements on a conveyor belt. But Wang [5], based upon video observations, recorded a quasi-linear velocity profile at the head of two-phase debris flow, while Jensen et al. [6] using a PIV technique observed a quasi-uniform velocity profile in wave runup on a steep beach.

Research into highly-unsteady gas-liquid flow situations has been very limited, with a few exceptions. These include studies of cavitating flows [7] and void fraction measurements in breaking waves [8]. Nearly all works were performed in periodic flows enabling repeated measurements.

During the present study, surging waters were investigated in a large-size channel with a rough invert consisting of a succession of abrupt drops. The results provide new information on the wave front propagation, while unsteady two-phase flow measurements were conducted to gain new insights into the air-water flow characteristics and momentum exchanges.

Experimental Setup

New experiments were performed in the 24 m long 0.5 m wide flume with a slope $S_o \sim 0.065$ ($\theta = 3.4°$) previously used by Chanson [9]. A precise flow rate was delivered by a pump controlled with an adjustable frequency AC motor drive Taian T-Verter K1/N1 (Pulse Width Modulated design), enabling an accurate discharge adjustment in a closed-circuit system. The flow was fed through a smooth convergent nozzle (1.7 m long), and the nozzle exit was 30 mm high and 0.5 m wide. The chute consisted of a 2.4 m long horizontal section, immediately downstream of the nozzle, followed by 18 identical abrupt drops (h = 0.0715 m), each followed by a 1.2 m long horizontal step.

(A) Lake Ha!Ha! Canada, July 1996 - Looking upstream at the breached dam (Courtesy of Natural Resources Canada)

(B) Present study: Q(t=0+) = 0.065 m^3/s, step 16, looking at advancing surge (Courtesy of C.G. SIM and C.C. TAN)

Fig. 1 - Photographs of dam break and resulting surging wave.

Instrumentation

The flow rates in steady flow conditions were measured with a Dall tube flowmeter, calibrated on site with a sharp-crested weir, with an accuracy of about 2%. The surging flow was studied with high-shutter speed digital still- and video-cameras.

Air-water flow properties were measured with two systems. Air concentrations and bubble count rates were recorded with an

array of single-tip conductivity probes (needle probe design). Each probe consisted of a sharpened rod (∅ = 0.35 mm) which was insulated except for its tip and set into a metal supporting tube acting as the second electrode. The second apparatus was a double-tip conductivity probe. The inner electrode was a Platinum wire (∅ = 0.15 mm) and the outer electrode was a stainless steel surgical needle (∅ = 0.5 mm). Each tip was identical and the distance between sensors was Δx_{tip} = 8.9 mm. With both probe systems, the sensors were aligned along the flow direction and excited by an air bubble detector developed at the University of Queensland (UQ82.518) with a response time of less than 10 μs and calibrated with a square wave generator. The probe output signals were scanned at 10 kHz per channel.

Data acquisition was triggered manually immediately prior to the flow arrival to have a minimum of 5 seconds of record. Visual observations showed that the wave front was roughly two-dimensional, and measurements were conducted on the centreline at several distances x from the step vertical face. At most locations, a single-tip conductivity probe (i.e. reference probe) was set on the invert, acting as a time reference, while the other probes were set at different elevations. In the free-jet region, the reference probe was set at the brink height (i.e. y = h) to investigate the jet flow. Each experiment was repeated until sufficient data were obtained for each vertical profile.

The displacement of the probes in the vertical direction was controlled by a fine adjustment travelling mechanism with an error of less than 0.2 mm.

Data Processing

Video-taped movies were analysed frame-by-frame. The error on the time was less than 1/250 s and the error on the longitudinal position of the wave front was +/- 1 cm.

The conductivity probe signal outputs were processed using a single threshold technique. The threshold was set at 50% of air-water range. Unsteady void fractions C and bubble count rates F were calculated during a short time interval τ such as $\tau = \Delta X/V_s$ where V_s is the surge front celerity measured with the video-cameras and ΔX is the control volume streamwise length. Preliminary tests indicated that the control volume length had to satisfy $\Delta X \geq 70$ mm to contain a minimum of 5 to 20 bubbles [9]. The bubble count rate was calculated as: $F = N_{ab}/\tau$ where N_{ab} is the number of bubbles detected during the time interval τ.

Velocity data were calculated from individual droplet/bubbles events impacting successively the two probe sensors. The velocity was deduced from the time lag δt for air-to-water interface detections by both leading and trailing tips respectively. For each meaningful event, the interfacial velocity was calculated as: $V = \Delta x_{tip}/\delta t$ where Δx_{tip} is the distance between probe sensor. The processing technique was compared successfully with video-observations of the shock front celerity and with the speed of ejected droplets.

Boundary conditions

Before each run, the recirculation pipe system and convergent intake were emptied, while the channel was dry. The pump was rapidly started and reached nominal discharge Q(t=0+) in 5 sec.: that is, at least 10 sec. prior to the waters entering the channel. The discharge Q(t=0+) was maintained constant until the experiment end. Experiments were conducted for Q(t=0+) = 0.050, 0.060, 0.065 and 0.070 m^3/s.

For completeness, preliminary tests were conducted with the channel initially dry and wet. Visual observations demonstrated a major change in wave front shape in the presence of an initial film of water. Indeed, in presence of an initial water skin, the wave front was led by a positive surge that is completely different from surging waters on a dry bed [10,11].

Basic Observations

For all flow conditions, visual observations and void fraction data demonstrated that the surging waters propagated as a succession of free-falling nappe, nappe impact and horizontal runoff (Fig. 2). At each step brink, the advancing surge took off as a free-jet, before impacting onto the downstream step around x = 0.2 to 0.3 m. Nappe impact was associated with very significant spray and splashing, with water droplets reaching heights in excess of 0.5 m. Further, waters started to fill the cavity beneath the nappe, and the cavity became drowned after sometimes. The cavity filling process was however relatively slow compared to the surge propagation on each step. Downstream of nappe impact, the advancing waters ran off the step as a surge wave on dry bed.

The wave leading edge was highly aerated, in particular for the larger flow rates (Fig. 1B). Figure 1B emphasises the chaotic nature of wave front, with strong spray, splashing and wavelets. Water packets were commonly projected to heights greater than 3 to 5 step heights, while some droplets reached heights of more than 10 step heights. Visually laboratory experiments in the large-size flume had a similar appearance to prototype surging flows observed on Brushes Clough dam spillway and in Glashütte township.

The propagation of the wave front was recorded for a range of unsteady flow conditions. Wave front celerity data showed some flow acceleration in the first 4 to 6 steps. Further downstream, a gradual decay in celerity V_s was observed. The data were compared successfully with Hunt's [12] theory for dam break wave down sloping chutes. A fair agreement was achieved assuming an equivalent Darcy-Weisbach friction factor f = 0.05, irrespective of flow rate and chute configuration [4, Present study]. This flow resistance value is close to air-water flow measurement results in steady flow conditions yielding f ~ 0.047 [13].

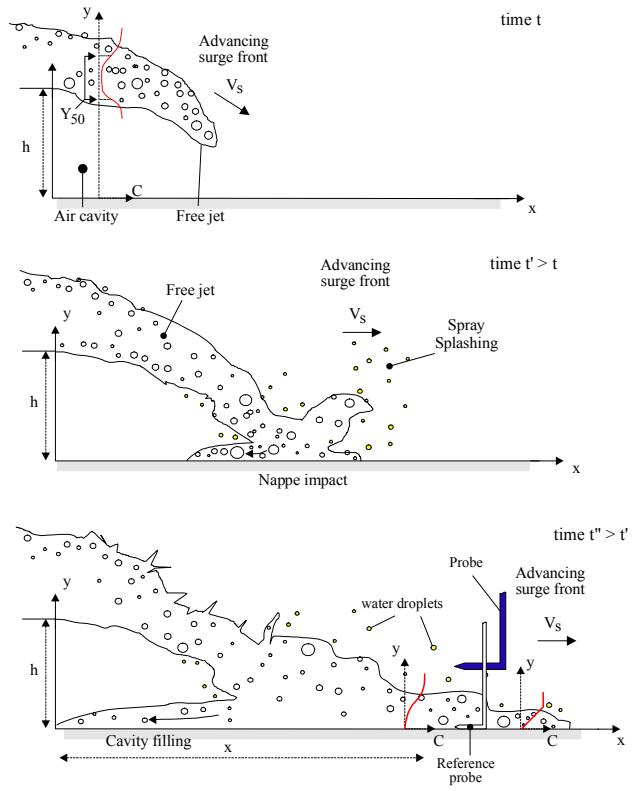

Fig. 2 - Definition sketch of advancing surging downstream of an drop.

Void Fractions and Bubble Count Rate Distributions

Quasi-instantaneous measurements of void fractions in the free-

jet and in the horizontal runoff are presented in Figures 3 and 4 respectively. In each figure, instantaneous distributions for different times t are shown at a given location x, where t is the time from the first water detection by the reference probe. In Figures 3 and 4, the vertical axis is y/d_o where y is the vertical coordinate and d_o is a measure of the initial flow rate Q(t=0+) :

$$d_o = \frac{9}{4}\sqrt[3]{\frac{Q(t=0+)^2}{g\,W^2}} \qquad (1)$$

g is the gravity acceleration and W is the chute width.

In the free-jet region (i.e. x < 0.2 to 0.3 m), interfacial aeration occurred at both upper and lower nappes. Instantaneous distributions of void fraction followed closely analytical solutions of the air bubble diffusion equation for upper and lower nappes :

$$C = \frac{1}{2}\left(\text{erf}\left(\frac{y - Y_{50}}{2\sqrt{\frac{D_t}{V_s}x}}\right) - 1\right) \qquad (2A)$$

$$C = \frac{1}{2}\left(1 - \text{erf}\left(\frac{y - Y_{50}}{2\sqrt{\frac{D_t}{V_s}x}}\right)\right) \qquad (2B)$$

where C is the void fraction, Y_{50} are the characteristic locations where C = 0.50 in the nappe, D_t is an air bubble diffusivity, V_s is the surge front celerity, and the function erf is the Gaussian error function :

$$\text{erf}(u) = \frac{2}{\sqrt{\pi}} * \int_0^u \exp(-v^2)\,dv \qquad (3)$$

Equations (2A) and (2B) were developed respectively for the upper and lower nappes of steady water jets, assuming constant bubble diffusivity [14,15]. They are compared with experimental data in Figure 3. The results show an increase in nappe thickness with increasing time at a given location. Note the start of cavity filling in Figure 3B.

In the nappe impact region and in the horizontal runoff, the void fraction distributions at the leading edge of the surging waters had a quasi-linear shape :

$$C = 0.9\frac{y}{Y_{90}} \qquad t\sqrt{g/d_o} < 1.0 \quad (4)$$

where Y_{90} is the height where C = 0.90. For larger times (i.e. $t\sqrt{g/d_o} > 1.5$), the distributions of air concentration exhibited an inverted S-shape that was best described by the diffusion model :

$$C = 1 - \tanh^2\left(K' - \frac{\frac{y}{Y_{90}}}{2\,D_o} + \frac{\left(\frac{y}{Y_{90}} - \frac{1}{3}\right)^3}{3\,D_o}\right) \qquad (5)$$

where K' and D_o are functions of the depth-averaged void fraction C_{mean} only [16].

Typical instantaneous void fraction data are presented in Figure 4, in which they are compared with Equations (4) and (5). These are analytical solutions of the advective diffusion of air bubbles assuming respectively the following distributions of dimensionless turbulent diffusivity of air bubbles:

$$D' = \frac{C\sqrt{1 - C}}{0.9} \qquad t\sqrt{g/d_o} < 1.0 \quad (6)$$

$$D' = D_o\left(1 - 2\left(\frac{y}{Y_{90}} - \frac{1}{3}\right)^2\right)^{-1} \qquad t\sqrt{g/d_o} > 1.5 \quad (7)$$

where $D' = D_t/((u_r)_{Hyd}.\cos\theta.Y_{90})$, $(u_r)_{Hyd}$ is the bubble rise velocity in hydrostatic pressure gradient. Note that the shape of Equation (7) is similar to the sediment diffusivity distribution which yields to the Rouse distribution of suspended matter.

Bubble count rate data showed systematically large bubble count rates, hence large interfacial areas, at the surge leading edge, while the maximum bubble count rates tended to decrease with increasing time t towards steady flow values.

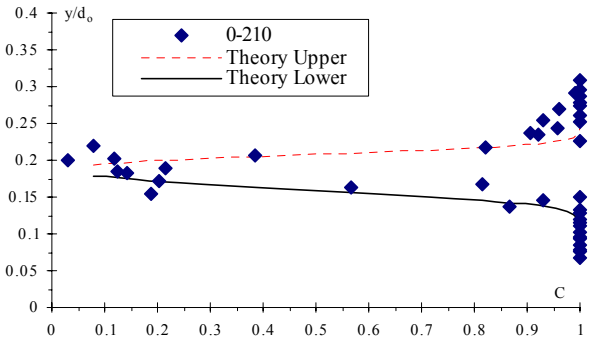

(A) t = 0.044 s, ΔX = 0.21 m

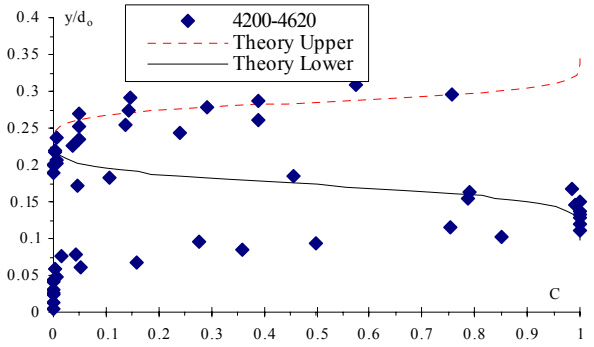

(B) t = t = 1.87 s, ΔX = 0.42 m - Note the start of cavity filling

Fig. 3 - Dimensionless distributions of instantaneous void fractions in the free-jet flow region (Q(t=0+) = 0.070 m^3/s, d_o = 0.283 m, , step 16, x = 0.1 m, V_s = 2.36 m/s) - Comparison with Equations (2A) and (2B)

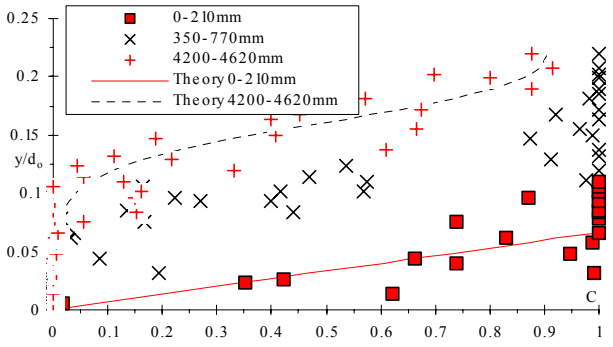

Fig. 4 - Dimensionless distributions of instantaneous void fractions in the horizontal runoff region (Q(t=0+) = 0.070 m^3/s, d_o = 0.283 m, V_o = 0.48 m/s, step 16, x = 0.8 m, V_s = 2.57 m/s) - t = 0.040 [0-210], 0.210 [350-770], 1.66 s [4200-4620].

Velocity Distributions

In the free-jet region (x < 0.3 m), velocity distributions showed a quasi-uniform profile. Despite some scatter, the data suggested a reasonably uniform velocity distribution, although some high-speed water projections were observed in the initial instants.

Figure 5 presents typical instantaneous velocity data in the horizontal runoff region. Each data point represents the velocity of the first air-to-water interface at each position y. At the surge leading edge, the instantaneous velocity data compared reasonably well with an analytical solution of the Navier-Stokes equations (first Stokes problem) for startup flow (Fig. 5):

$$\frac{V}{U} = \text{erf}\left(\frac{y}{2\sqrt{\nu_T\, t}}\right) \qquad (8)$$

where U is a free-stream velocity, t is the time, and ν_T is the momentum exchange coefficient. Dimensionless distributions of time-average velocity (over about 5 sec.) were typically quasi-uniform suggesting a potential flow region above the shear zone. The magnitude of time-average velocities was consistently smaller than the velocity of the first interface, possibly because of water projections ahead of the surging waters. The data further highlighted high levels of turbulence in the surging flow, with turbulence levels ranging from 20 to 100% with mean values of about 50%. These were consistent with observed turbulence levels in steady stepped chute flows [16,17].

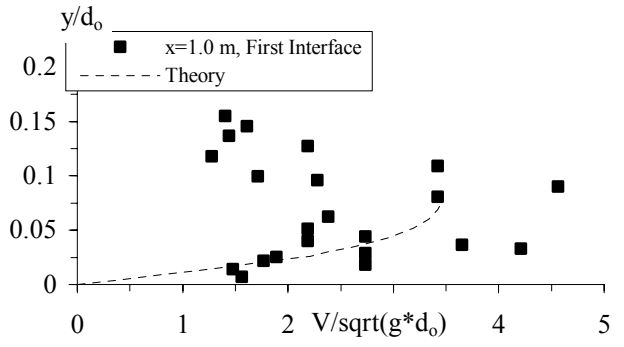

Fig. 5 - Instantaneous velocity distributions at surge leading edge in horizontal runoff (Q(t=0+) = 0.065 m^3/s, d_o = 0.27 m, step 16, x = 1.0 m) - Interfacial velocity of first air-to-water interface (t < 0.12 s) - Comparison with Equation (8).

Discussion

In the horizontal runoff flow, the data highlighted a boundary layer region next to the invert in the shock front (Fig. 5). The finding is consistent with earlier laboratory experiments [3,4]. The values of U and ν_T (Eq. (8)) were determined from best data fit. Despite some scatter and crude approximations leading to Equation (8), the results implied a turbulent boundary layer.

Based upon present void fraction and velocity measurements in horizontal runoff flow, the air bubble diffusivity D_t and eddy viscosity ν_T which satisfy Equations (4) and (8) respectively yielded a ratio D_t/ν_T of about unity in the surge front. The ratio D_t/ν_T compares the effects of the difference in diffusion of a discrete bubble particle and small coherent fluid structure, as well as the effect of entrained air on the turbulence field. The result $D_t/\nu_T \sim 1$ seems to suggest strong interactions between air bubble diffusion and momentum exchange processes.

Conclusion

New experiments were conducted systematically in surging waters down a 24 m long chute with a succession of abrupt drops. Unsteady air-water flow measurements were performed in the surging waters using an array of conductivity probes. Visual observations showed that the surges propagated at a succession of free jets immediately downstream of each abrupt drop, nappe impact and horizontal runoff flow. The results showed quantitatively a strong aeration of surge leading edge. The void fraction distributions followed reasonably well analytical solutions of air bubble diffusion equation developed for steady flow conditions. In the horizontal runoff, velocity data showed the presence of an unsteady turbulent boundary layer next to the invert. Overall the results emphasised the complicated nature of the surging flow and its front.

It must be emphasised that present results were focused on a flat chute (3.4°) in which the horizontal runoff was a dominant flow motion. On steeper slopes, preliminary observations suggested significantly more complicated processes.

Acknowledgments

The writer thanks his students Chye-guan SIM, and Chee-chong TAN for their help and assistance.

References

[1] Dressler, R., Comparison of Theories and Experiments for the Hydraulic Dam-Break Wave, *Proc. Intl Assoc. of Scientific Hydrology* Assemblée Générale, Rome, Italy, 1954, **3** (38), pp. 319-328.

[2] Escande, L., Nougaro, J., Castex, L., and Barthet, H., Influence de Quelques Paramètres sur une Onde de Crue Subite à l'Aval d'un Barrage." *Jl La Houille Blanche*, 1961, (5) pp. 565-575.

[3] Mano, A., Boundary Layer Developed near Surging Front." *Coastal Engineering in Japan*, 1994, **37** (1) pp. 23-39.

[4] Fujima, K., and Shuto, N., Formulation of Frictions Laws for Long Waves on a Smooth Dry Bed, *Coastal Engineering in Japan*, 1990, **33** (1) pp. 25-47.

[5] Wang, Z.Y., Initiation and Mechanism of Two Phase Debris Flow." *Proc. Conf. on Flood Defence'2002*, Ed. Wu et al., Science Press, New York, 2002, pp. 1637-1648.

[6] Jensen, A., Pedersen, G.K., and Wood, D.J., An Experimental Study of Wave Run-up on a Steep Beach, *Jl of Fluid Mech.*, 2003, **486** pp. 166-188.

[7] Stutz, B., and Reboud, J.L., Measurements within Unsteady Cavitation." *Experiments in Fluids*, 2000, **29** pp. 545-552.

[8] Hwung, H.H., Chyan, J.M., and Chung, Y.C., Energy Dissipation and Air Bubbles Mixing inside Surf Zone." *Proc. 23rd Intl Conf. on Coastal Eng.*, ASCE, Venice, Italy, 1992, **1** (22) pp. 308-321.

[9] Chanson, H, Sudden Flood Release down a Stepped Cascade. Unsteady Air-Water Flow Measurements. Applications to Wave Run-up, Flash Flood and Dam Break Wave, *Report CH51/03*, Dept of Civil Eng., Univ. of Queensland, Brisbane, Australia, 142 pages, 2003.

[10] Henderson, F.M, *Open Channel Flow*, MacMillan Company, New York, USA, 1966.

[11] Montes, J.S., *Hydraulics of Open Channel Flow*, ASCE Press, New-York, USA, 697 pages, 1998.

[12] Hunt, B., Asymptotic Solution for Dam-Break Problems, *Jl of Hyd. Div.*, Proceedings, ASCE, 1982, **108** (HY1) pp. 115-126.

[13] Chanson, H., and Toombes, L., Energy Dissipation and Air Entrainment in a Stepped Storm Waterway: an Experimental Study, *Jl of Irrigation and Drainage Engrg.*, ASCE, 2002, **128** (5) pp. 305-315.

[14] Chanson, H., Study of Air Entrainment and Aeration Devices, *Jl of Hyd. Res.*, IAHR, 1989, **27** (3) pp. 301-319.

[15] Brattberg, T., Chanson, H., and Toombes, L., Experimental Investigations of Free-Surface Aeration in the Developing Flow of Two-Dimensional Water Jets, *Jl of Fluids Eng.*, Trans. ASME, 1998, **120** (4) pp. 738-744.

[16] Chanson, H., and Toombes, L., Strong Interactions between Free-Surface Aeration and Turbulence down a Staircase Channel, *Proc. 14th Australasian Fluid Mech. Conf.*, Adelaide, Australia, 2001, pp. 841-844

[17] Ohtsu, I., and Yasuda, Y., Characteristics of Flow Conditions on Stepped Channels, *Proc. 27th IAHR Biennal Congress*, San Francisco, USA, 1997, Theme D, pp. 583-588.